

Unitary and Analytic Models in Particle Physics Phenomenology¹

S.Dubnička

Institute of Physics, Slovak Academy of Sciences, Dúbravská cesta 9, 842 28 Bratislava,
Slovak Republic

A.Z. Dubničková

Dept. of Theor. Physics, Comenius University, Mlynská dolina, 842 48 Bratislava, Slovak
Republic

Pavol Stríženec

Institute of Exp. Physics, Slovak Academy of Sciences, Košice, Slovak Republic

Abstract

After two decades of a development of the unitary and analytic models of the electromagnetic structure of hadrons and nuclei their main principles are briefly formulated, then a general scheme of their applications to the electromagnetic, weak and strong interaction processes are traced out and finally, some results of their successful applications are reviewed.

1 Introduction

Hadrons are compound of quarks and as a result, they manifest a structure in electromagnetic, weak and strong interactions which makes complications at a description of various processes with hadrons by standard quantum-field theoretical approaches.

The latter problem in electromagnetic and weak interactions of hadrons was solved by an introduction of functions of one variable, so-called form factors (FF's) of hadrons, being coefficients in a decomposition of the unknown hadronic matrix element of the corresponding current into a maximum number of linearly independent covariants constructed of four-momenta and spin parameters of the hadron under consideration. Their behaviour is expected to be predicted by the fundamental theory of quark-gluon interactions, QCD.

¹*Contribution presented at the International Hadron Structure 2000 Conference held on October 2-7, 2000 in Stará Lesná, High Tatra Mountains, Slovak Republic*

However, we know, that merely at sufficiently small distances (thanks to its asymptotic freedom) QCD becomes a weakly coupled quark-gluon theory to be amenable to a perturbative expansion in the running coupling constant α_s and predicts just the asymptotic behaviour of FF's. In low momentum transfer region, where α_s becomes large, the quark-gluon perturbation theory breaks down and non-perturbative methods in QCD are not well worked out to give interesting results on the FF's of hadrons. The same is valid also for the low energy time-like region where FF's acquire the most complicated, resonant, behaviour. In this contribution we would like to present the phenomenological unitary and analytic approach which compensates abovementioned problems to some extent and renders possible to achieve a line of interesting results.

2 Subject of our interest

The effectuality of our phenomenological approach will be demonstrated mainly on binary processes caused by electromagnetic, weak and strong interactions, though also weak decays of τ -lepton into two pseudoscalar mesons are useful to be considered. The worked out unitary and analytic models depend on some number of unknown parameters, which can be evaluated practically in a comparison of the model under consideration with a corresponding experimental information. Therefore first, we concentrate our attention to the *electromagnetic* processes of the type $e^+e^- \rightarrow h\bar{h}$ and $e^-h \rightarrow e^-h$, $h = P(\pi, K), B(N, \Lambda, \Sigma, \Xi)$, where on π, K and N the abundant experimental information exists. These processes are described by the cross-sections

$$\sigma^{\text{c.m.}}(e^+e^- \rightarrow P\bar{P}) = \frac{\pi\alpha^2}{3t}\beta_P^3(t)|F_P(t)|^2 \quad (1)$$

$$\sigma^{\text{c.m.}}(e^+e^- \rightarrow B\bar{B}) = \frac{4\pi\alpha^2}{3t}\beta_B(t) \left[|G_M^B(t)|^2 + \frac{2m_B^2}{t}|G_E^B(t)|^2 \right] \quad (2)$$

and

$$\begin{aligned} \frac{d\sigma^L(e^-P \rightarrow e^-P)}{d\Omega} &= \frac{\alpha^2}{4E^2} \cdot \frac{\cos^2\theta/2}{\sin^4\theta/2} \cdot \frac{1}{1 + \frac{2E}{m_P}\sin^2\theta/2} \cdot F_P^2(t) \\ \frac{d\sigma^L(e^-B \rightarrow e^-B)}{d\Omega} &= \frac{\alpha^2}{4E^2} \cdot \frac{\cos^2\theta/2}{\sin^4\theta/2} \cdot \frac{1}{1 + \frac{2E}{m_B}\sin^2\theta/2} \cdot \\ &\cdot \left[(F_1^B(t))^2 - \frac{t}{4m_B^2}(F_2^B(t))^2 - 2\frac{t}{4m_B^2}(F_1^B(t) + F_2^B(t))^2 \text{tg}^2\theta/2 \right] \end{aligned} \quad (3)$$

with α -the fine structure constant, $\beta_{P,B}(t) = \sqrt{\frac{t-4m_{P,B}^2}{t}}$; $t = -Q^2$ momentum transfer squared, where

$$G_E^B(t) = F_1^B(t) + \frac{t}{4m_B^2} F_2^B(t) \quad (4)$$

$$G_M^B(t) = F_1^B(t) + F_2^B(t).$$

All dynamics of the processes $e^+e^- \rightarrow h\bar{h}$ and $e^-h \rightarrow e^-h$ is comprised in the functions of one variable $F_P(t)$, $F_1(t)$, $F_2(t)$, $G_E^B(t)$, $G_M^B(t)$, the so-called electromagnetic form factors (FF's) of hadrons.

Next we shall be interested in the *weak* processes of the type $\bar{\nu}_e e^- \rightarrow P^0 P^-$ ($P = \pi, K$) and $\tau^- \rightarrow \nu_\tau P^0 P^-$, described by the cross-section

$$\sigma(\bar{\nu}_e e^- \rightarrow P^0 P^-) = \frac{G_F^2}{48\pi} t \beta_P^3 |F_P^W(t)|^2 \quad (5)$$

and the partial decay width expression

$$\Gamma(\tau^- \rightarrow \nu_\tau P^0 P^-) = \frac{G_F^2 \cos^2 \Theta_c}{384\pi^3 m_\tau^3 C_P^2} \int_{4m_\pi^2}^{m_\tau^2} dt (m_\tau^2 - t)(m_\tau^2 + 2t) \beta_P^3 |F_P^W(t)|^2, \quad (6)$$

respectively, where G_F is the Fermi coupling constant of weak interactions, $\Theta_c \approx 13^\circ$ is the Cabibbo angle, $C_\pi = \sqrt{2}$ and $C_K = 2$. Again all dynamics of the processes $\bar{\nu}_e e^- \rightarrow P^0 P^-$ and $\tau^- \rightarrow \nu_\tau P^0 P^-$ is comprised in the weak FF's $F_P^W(t)$. Finally, one can consider also *strong* binary processes of the type $a + a \rightarrow a + a$; $a + b \rightarrow a + b$ and $a + b \rightarrow c + d$ to be described generally by the cross-section

$$\frac{d\sigma^{\text{c.m.}}(a + b \rightarrow c + d)}{d\Omega} = \frac{\pi^2 q}{4s p} \frac{1}{(2S_a + 1)(2S_b + 1)} \sum_{\lambda_a \lambda_b \lambda_c \lambda_d} |T_{cd;ab}^{(s)}(s, t)|^2, \quad (7)$$

where $T_{cd;ab}^{(s)}(s, t)$ is the s -channel c.m. helicity amplitude, $p = |\vec{p}_a| = |\vec{p}_b|$; $q = |\vec{p}_c| = |\vec{p}_d|$; s -is total c.m. energy squared, S_a, S_b, S_c, S_d are spins and $\lambda_a, \lambda_b, \lambda_c, \lambda_d$ spin projections of a, b, c, d particles, respectively. If elastic scattering of two spin-zero particles is considered and a redefinition of the amplitude

$$T(s, t) = -\frac{1}{4\pi^2} M(s, t) \quad (8)$$

is taken into account, equation (7) becomes

$$\frac{d\sigma}{d\Omega} = \frac{1}{64\pi^2 s} |M(s, t)|^2. \quad (9)$$

Then one can define the total cross-section by the relation

$$\sigma_{\text{tot}}^{(s)} = \int \frac{d\sigma}{d\Omega} d\Omega. \quad (10)$$

As a consequence of the conservation of angular momentum, the scattering amplitude $M(s, t)$ can be expanded in a series of partial wave amplitudes $f_l(s)$ as functions of only one variable

$$M(s, t) = \sum_{l=0}^{\infty} (2l + 1) f_l(s) P_l(\cos \theta) \quad (11)$$

where θ is the c.m. scattering angle and $P_l(\cos \theta)$ are the Legendre polynomials. For a general case of particles with non-zero spin and unequal masses the expansion of helicity amplitudes in (7) is exactly analogous to eq. (11), except that l is replaced by the total angular momentum J and the Legendre polynomials $P_l(\cos \theta)$ by the rotation Wigner's functions $d_{\lambda\mu}^J(\theta)$. Here all dynamics of the processes $a + a \rightarrow a + a$, $a + b \rightarrow a + b$ and $a + b \rightarrow c + d$ is comprised in the partial wave amplitudes $f_l(s)$. The eq. (11) has enormous practical importance as at low energies only low partial waves give non negligible contributions so that the scattering amplitude may be well approximated by a severely truncated partial wave series.

3 Common features of considered electromagnetic, weak and strong processes

One could notice that all considered electromagnetic, weak and strong interaction processes are completely described provided that the corresponding functions (electromagnetic and weak FF's and the partial wave amplitudes) of one variable are known explicitly. Here we review their three basic properties, which enable us then to construct for them realistic phenomenological models.

- i) Experimentally measured total cross-sections (in τ -decay it is invariant mass distribution) as functions of the energy manifest sharp variations associated with an occurrence of unstable objects, resonances, characterized by the mass m_r and the width Γ_r , where the latter is related to the life-time τ_r of the resonance by the relation

$$1/\Gamma_r \approx \tau_r \sim 10^{-23} \text{s}.$$

This property is automatically transferred into the absolute values of corresponding FF's and partial wave amplitudes, and in a construction of models for the latter

functions of one variable this experimental fact has to be taken into account in the first place.

- ii) Electromagnetic and weak FF's, as well as partial wave amplitudes of strong interaction processes, are analytic functions in the whole complex plane of their argument, except for isolated singularities. In the case of electromagnetic and weak FF's of hadrons they are branch points on the positive real axis corresponding to *normal* (given by the unitarity condition) and *anomalous* (given by allowed triangle diagrams) thresholds generating many-sheeted Riemann surface. The first sheet is called physical, all other sheets of the Riemann surface are unphysical. In the case of partial wave amplitudes of strong interaction binary processes the situation is even more complex and depends on the fact, if there is scattering of particles of

- equal masses ($a + a \rightarrow a + a$):

The cuts on the positive real axis are similar as for electromagnetic and weak FF's. Besides the latter there is also left-hand cut from $-\infty$ to $s = 0$.

- unequal masses ($a + b \rightarrow a + b$): $m_b > m_a$

On the positive real axis there are unitary cuts similar with those of electromagnetic and weak FF's. Besides the latter there is the short cut between $(m_b^2 - m_a^2/m_b^2)$ and $(m_b^2 + 2m_a^2)$, left-hand cut from $-\infty$ to $(m_b - m_a)^2$ and circular cut with a center at the origin and the radius equal to $(m_b^2 - m_a^2)$.

- 4 different particles ($a + b \rightarrow c + d$):

The situation is very complicated and it is out of the scope of our interest.

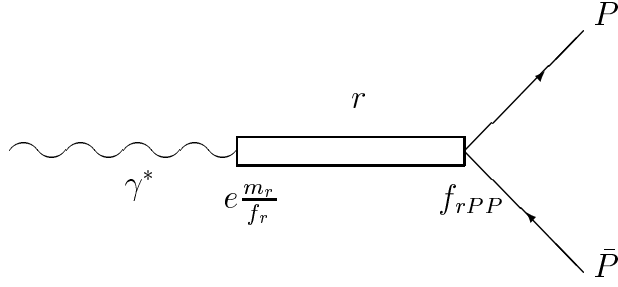
Generally, the partial wave amplitude can be written as a quotient of two functions

$$f_l(s) = N_l(s)/D_l(s) \tag{12}$$

in such a way that $D_l(s)$ contains only the right-hand unitary cuts and $N_l(s)$ only the left-hand cuts of $f_l(s)$. Any s -channel resonance in electromagnetic and weak FF's, as well as in the partial wave amplitudes of strong interaction processes, is always associated with a pair of complex conjugate poles on unphysical sheets to be generated by the branch points on the positive real axis of the s -plane.

- iii) Asymptotic behaviour of electromagnetic and weak FF's is related to the number of constituent quarks n_q of the hadron under consideration by means of the expression

$$F_h(t)|_{|t| \rightarrow \infty} \sim t^{n_q - 1} \tag{13}$$



i.e.

$$F_P(t)|_{|t|\rightarrow\infty} \sim \frac{1}{t}; \quad G_{E,M}^B(t)|_{|t|\rightarrow\infty} \sim \frac{1}{t^2}. \quad (14)$$

The cross-section of the process $a + b \rightarrow a + b$ behaves asymptotically as follows

$$\frac{d\sigma(a + b \rightarrow a + b)}{dt}|_{s\rightarrow\infty} \sim \frac{1}{s^n} f(t/s) \quad (15)$$

where $n = 2(n_a + n_b - 1)$ and n_a, n_b are numbers of the constituent quarks of a, b particles.

4 The main idea of construction of unitary and analytic models

In the previous section on the base of observation of the experimentally measured total cross-sections we have been driven to the idea that all electromagnetic and weak FF's of hadrons are formed by a contribution of unstable resonant states, completely described by m_r, Γ_r and residuum, and a smooth background generated by unitary cuts on the positive real axis. In the case of the partial wave amplitudes a smooth background of the latter type is enlarged by $N_l(s)$ contributions of the left-hand cuts.

Therefore, now, it is straightforward to demonstrate a procedure how to unify consistently the experimental fact of a creation of resonant states together with the assumed analytic properties and the asymptotic behaviour into one analytic function defined on four-sheeted Riemann surface with complex conjugate pairs of poles, corresponding to resonances, placed on unphysical sheets. For a simplicity, first we restrict ourselves to the electromagnetic FF's of pseudoscalar mesons P . In this case any resonance can be represented by the diagram (see above) to which the following pole expression

$$\frac{m_r^2}{m_r^2 - t} (f_{rPP}/f_r) \quad (16)$$

corresponds, where f_{rPP} is the coupling constant of the resonance to the pseudoscalar meson P and f_r is the coupling constant describing the photon-vector-meson transition. The pole expression (16) has the asymptotics $\sim 1/t$. In order to transform (16) into one analytic function

- i) with two square-root branch points on the positive real axis
- ii) with two pairs of complex conjugate poles on unphysical sheets corresponding to the resonance r

one proceeds as follows:

- first, the nonlinear transformation

$$t = t_0 + \frac{4(t_{in} - t_0)}{[1/W(t) - W(t)]^2} \quad (17)$$

with t_0 - the square-root branch point corresponding to the lowest threshold and t_{in} - an effective square-root branch point simulating contributions of all other relevant thresholds given by the unitarity condition is applied, which automatically generates the relations

$$m_r^2 = t_0 + \frac{4(t_{in} - t_0)}{[1/W_{r0} - W_{r0}]^2} \quad (18)$$

and

$$0 = t_0 + \frac{4(t_{in} - t_0)}{[1/W_N - W_N]^2} \quad (19)$$

- then relations between W_{r0} and W_{r0}^* are utilized
- and finally, the instability of the resonance is introduced by its non-zero width $\Gamma_r \neq 0$.

The application of the (17)-(19) to (16) leads to the following factorized form

$$\begin{aligned} \frac{m_r^2}{m_r^2 - t} (f_{rPP}/f_r) &= \left(\frac{1 - W^2}{1 - W_N^2} \right)^2 \cdot \\ &\cdot \frac{(W_N - W_{r0})(W_N + W_{r0})(W_N - 1/W_{r0})(W_N + 1/W_{r0})}{(W - W_{r0})(W + W_{r0})(W - 1/W_{r0})(W + 1/W_{r0})} \cdot \\ &\cdot (f_{rPP}/f_r) \end{aligned} \quad (20)$$

with asymptotic term (the first term, completely determining the asymptotic behaviour of (16)) and on the so-called finite-energy term (for $|t| \rightarrow \infty$ it turns out to be a real constant) giving a resonant behaviour around $t = m_r^2$. One can prove:

$$\text{a) if } m_r^2 - \Gamma_r^2/4 < t_{in} \Rightarrow W_{r0} = -W_{r0}^*$$

(21)

$$\text{b) if } m_r^2 - \Gamma_r^2/4 > t_{in} \Rightarrow W_{r0} = 1/W_{r0}^*$$

which lead the eq. (20) in the case a) to the expression

$$\begin{aligned} \frac{m_r^2}{m_r^2 - t} (f_{rPP}/f_r) &= \left(\frac{1 - W^2}{1 - W_N^2} \right)^2 \cdot \\ &\cdot \frac{(W_N - W_{r0})(W_N - W_{r0}^*)(W_N - 1/W_{r0})(W_N - 1/W_{r0}^*)}{(W - W_{r0})(W - W_{r0}^*)(W - 1/W_{r0})(W - 1/W_{r0}^*)} \cdot \\ &\cdot (f_{rPP}/f_r) \end{aligned} \quad (22)$$

and in the case b) to the following expression

$$\begin{aligned} \frac{m_r^2}{m_r^2 - t} (f_{rPP}/f_r) &= \left(\frac{1 - W^2}{1 - W_N^2} \right)^2 \cdot \\ &\cdot \frac{(W_N - W_{r0})(W_N - W_{r0}^*)(W_N + W_{r0})(W_N + W_{r0}^*)}{(W - W_{r0})(W - W_{r0}^*)(W + W_{r0})(W + W_{r0}^*)} \cdot \\ &\cdot (f_{rPP}/f_r). \end{aligned} \quad (23)$$

Lastly, introducing the non-zero width of the resonance by a substitution

$$m_r^2 \rightarrow (m_r - \Gamma_r/2)^2 \quad (24)$$

i.e. simply one has to get rid of "0" in sub-indices of (22) and (23), one gets:

in a) case

$$\begin{aligned} \frac{m_r^2}{m_r^2 - t} (f_{rPP}/f_r) &\rightarrow \left(\frac{1 - W^2}{1 - W_N^2} \right)^2 \cdot \\ &\cdot \frac{(W_N - W_r)(W_N - W_r^*)(W_N - 1/W_r)(W_N - 1/W_r^*)}{(W - W_r)(W - W_r^*)(W - 1/W_r)(W - 1/W_r^*)} \cdot \\ &\cdot (f_{rPP}/f_r) = \\ &= \left(\frac{1 - W^2}{1 - W_N^2} \right)^2 L(W_r)(f_{rPP}/f_r) \end{aligned} \quad (25)$$

and in b) case

$$\begin{aligned} \frac{m_r^2}{m_r^2 - t} (f_{rPP}/f_r) &\rightarrow \left(\frac{1 - W^2}{1 - W_N^2} \right)^2 \cdot \\ &\cdot \frac{(W_N - W_r)(W_N - W_r^*)(W_N + W_r)(W_N + W_r^*)}{(W - W_r)(W - W_r^*)(W + W_r)(W + W_r^*)} \cdot \\ &\cdot (f_{rPP}/f_r) = \\ &= \left(\frac{1 - W^2}{1 - W_N^2} \right)^2 H(W_r)(f_{rPP}/f_r) \end{aligned} \quad (26)$$

where no more equality can be used in (25) and (26) between the pole-term and the transformed expressions.

The latter are then analytic functions defined on four-sheeted Riemann surface, what can be seen explicitly by the inverse transformation to (17)

$$W(t) = i \frac{\sqrt{\left(\frac{t_{in}-t_0}{t_0}\right)^{1/2} + \left(\frac{t-t_0}{t_0}\right)^{1/2}} - \sqrt{\left(\frac{t_{in}-t_0}{t_0}\right)^{1/2} - \left(\frac{t-t_0}{t_0}\right)^{1/2}}}{\sqrt{\left(\frac{t_{in}-t_0}{t_0}\right)^{1/2} + \left(\frac{t-t_0}{t_0}\right)^{1/2}} + \sqrt{\left(\frac{t_{in}-t_0}{t_0}\right)^{1/2} - \left(\frac{t-t_0}{t_0}\right)^{1/2}}}. \quad (27)$$

These expressions have two pairs of complex conjugate poles on:

- a) case (25) - the second and fourth sheets
- b) case (26) - the third and fourth sheets,

describing always one resonance under consideration, and the asymptotic behaviour $\sim 1/t$, to be completely given by the asymptotic term $\left(\frac{1-W^2}{1-W_N^2}\right)^2$, more specifically, by its power "2". Here we would like also to note, that expressions (25) or (26) (it depends on the fact if the resonance is under the threshold t_{in} or above it) are more sophisticated analogues of the Breit-Wigner form and they can be applied to determine resonance parameters m_r , Γ_r from experimental data on pseudoscalar meson electromagnetic FF's in the region of the resonance under consideration.

As a result, the electromagnetic FF of any pseudoscalar meson can be represented by a sum of i -terms (25) of resonances below the threshold t_{in} and j -terms (26) of resonances above the threshold t_{in} as follows

$$F_P[W(t)] = \left(\frac{1-W^2}{1-W_N^2}\right)^2 \cdot \left\{ \sum_i \frac{(W_N - W_i)(W_N - W_i^*)(W_N - 1/W_i)(W_N - 1/W_i^*)}{(W - W_i)(W - W_i^*)(W - 1/W_i)(W - 1/W_i^*)} (f_{iPP}/f_i) + \sum_j \frac{(W_N - W_j)(W_N - W_j^*)(W_N + W_j)(W_N + W_j^*)}{(W - W_j)(W - W_j^*)(W + W_j)(W + W_j^*)} (f_{jPP}/f_j) \right\}, \quad (28)$$

which takes into account just $n = i + j$ resonances. It is analytic in the whole complex s -plane except for two cuts on the positive real axis and exhibits the asymptotic behaviour $\sim 1/t$.

If electromagnetic FF's of hadrons (like baryons and light nuclei) with more than $n_q = 2$ constituent quarks are considered and as a result FF's exhibit steeper falling in the asymptotic region, then in the construction of their unitary and analytic models one has to proceed as follows [1].

First, FF's are written down as a sum of finite number of pole expressions (16). Then the latter is by explicit requirements transformed to the form, which is automatically normalized and exhibits assumed asymptotic behaviour. And only then it is transformed by an application of the nonlinear transformation (17) to every pole term of FF to the unitary and analytic model with correct asymptotic behaviour. In this case a reduction of number of free parameters is achieved.

We note that knowing electromagnetic FF's of the hadron, by means of the conserved vector current (CVC) hypothesis one can predict the behaviour of the weak FF's of the same hadron.

Because the analytic properties of $D_l(s)$ function are of the same type as analytic properties of the electromagnetic and weak FF's, the above-prescribed procedure of a construction of the unitary and analytic models can be directly applied also to $1/D_l(s)$ function, which will be dominant in the partial wave amplitude considered in physical region.

5 Interesting results obtained by unitary and analytic models

5.1 Prediction of P-wave isovector $\pi\pi$ phase shift $\delta_1^1(s)$ and inelasticity $\eta_1^1(s)$ above inelastic threshold from $e^+e^- \rightarrow \pi^+\pi^-$ process.

The unitary and analytic model of $F_\pi^{EM}[W(s)]$ has one elastic cut $4m_\pi^2 < s < +\infty$ and one effective cut $s_{in} \approx 1\text{GeV}^2 < s < +\infty$. The elastic unitarity condition

$$\text{Im } F_\pi^{EM}(s) = F_\pi^{EM}(s) \cdot A_1^{1*}(s) \quad (29)$$

can be utilized for the analytic continuation of $F_\pi^{EM}[W(s)]$ through the elastic cut on the second Riemann sheet and as a result one obtains the FF on the II. sheet to be expressed by FF on the I. sheet and the $\pi\pi$ partial wave amplitude $A_1^1(s)$ on the I. sheet as follows

$$\left[F_\pi^{EM}(s) \right]^\text{II} = \frac{\left[F_\pi^{EM}(s) \right]^\text{I}}{1 + 2i \left[A_1^1(s) \right]^\text{I}} \quad (30)$$

from where

$$[A_1^1(s)]^I = \frac{[F_\pi^{EM}(s)]^I - [F_\pi^{EM}(s)]^{II}}{2i [F_\pi^{EM}(s)]^{II}} \quad (31)$$

to be valid in the whole complex s -plane. Now, substituting a standard parameterization

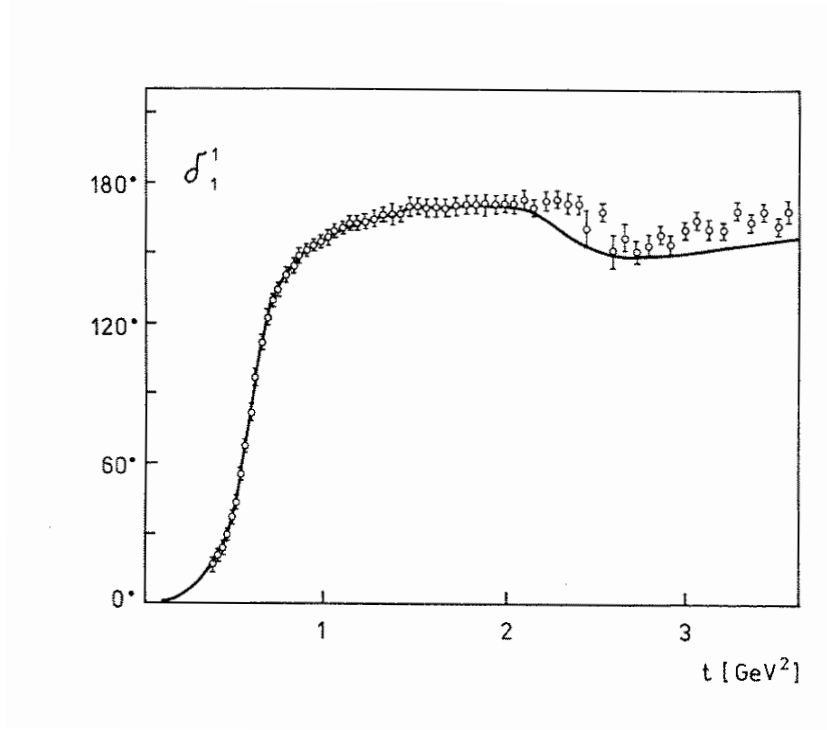


Figure 1:

of $I=J=1$ $\pi\pi$ scattering amplitude at the physical region

$$A_1^1(s + i\varepsilon) = \frac{\eta_1^1(s + i\varepsilon) e^{2i\delta_1^1(s+i\varepsilon)} - 1}{2i} \quad (32)$$

into (31) one gets

$$\eta_1^1(s + i\varepsilon) e^{2i\delta_1^1(s+i\varepsilon)} = \frac{[F_\pi^{EM}[W(s + i\varepsilon)]]^I}{[F_\pi^{EM}[W(s + i\varepsilon)]]^{II}} \quad (33)$$

from where it is straightforward to find

$$\delta_1^1(s + i\varepsilon) = \frac{1}{2} \operatorname{arctg} \frac{\operatorname{Im} \frac{[F_\pi^{EM}[W(s+i\varepsilon)]]^I}{[F_\pi^{EM}[W(s+i\varepsilon)]]^{II}}}{\operatorname{Re} \frac{[F_\pi^{EM}[W(s+i\varepsilon)]]^I}{[F_\pi^{EM}[W(s+i\varepsilon)]]^{II}}}; \quad \eta_1^1(s + i\varepsilon) = \left| \frac{[F_\pi^{EM}[W(s + i\varepsilon)]]^I}{[F_\pi^{EM}[W(s + i\varepsilon)]]^{II}} \right|. \quad (34)$$

Substituting unitary and analytic model of the pion electromagnetic FF in (34) one predicts [2] behaviour of $\delta_1^1(s + i\varepsilon)$ and $\eta_1^1(s + i\varepsilon)$ in a perfect agreement with existing data (see Figs.1 and 2) also in the inelastic region, i.e. above 1 GeV^2 .

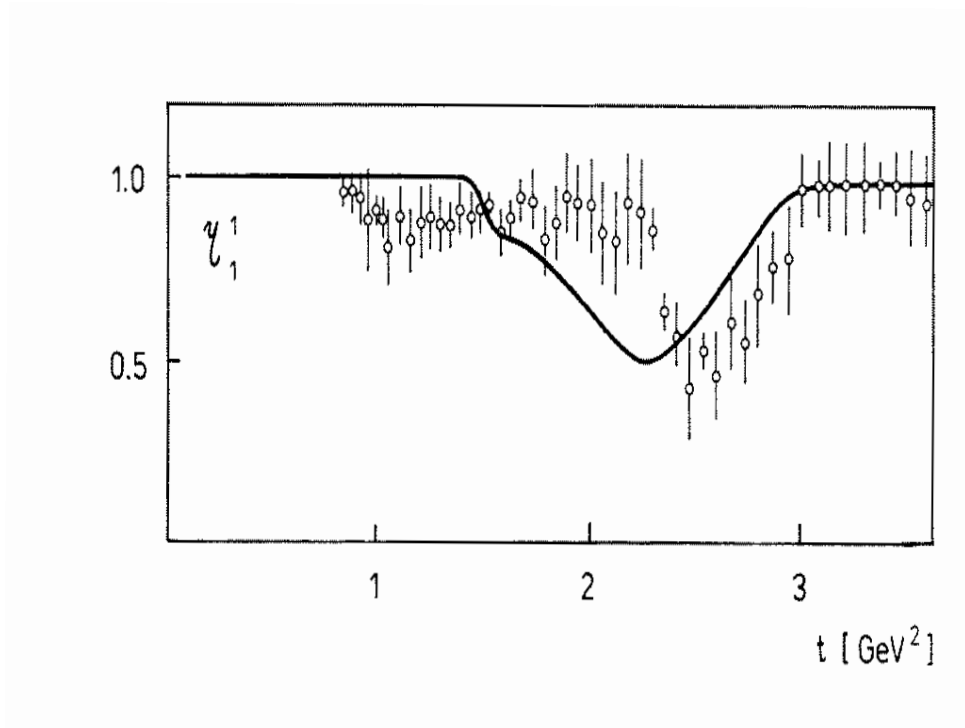


Figure 2:

5.2 Excited states of the $\rho(770)$ -meson

From Fig. 3, where the data on the pion electromagnetic FF are collected, one can see dominating role of the $\rho(770)$ -meson. Besides the latter one can notice in the data also another resonance around the energy $s = 2.9 \text{ GeV}^2$. But it does not mean at all there are no more other hidden ρ -resonances in the pion electromagnetic FF and the correct approach in an investigation of the latter problem is to take the expression (28), first, with two resonances, then with three resonances etc. and to look always for minimal value of χ^2 in experimental data fit.

Such a program was realized. Considering only two resonances in (28), $\chi^2/\text{NDF} = 539/279$ was achieved and $\rho(770)$ with $\rho''(1700)$ were identified. However, if three resonances were taken into account in (28), $\chi^2/\text{NDF} = 382/276$ was found and two excited states, $\rho'(1450)$ and $\rho''(1700)$, were detected [3]. Finally, by a consideration of four-resonances in (28), $\chi^2/\text{NDF} = 343/273$ was reached and in addition to $\rho'(1450)$ and $\rho''(1700)$, also the third excited state $\rho'''(2150)$ of the $\rho(770)$ -meson was revealed [4](see Fig. 4).

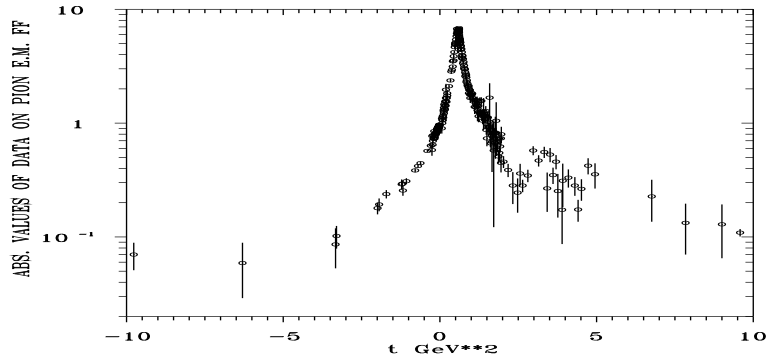


Figure 3:

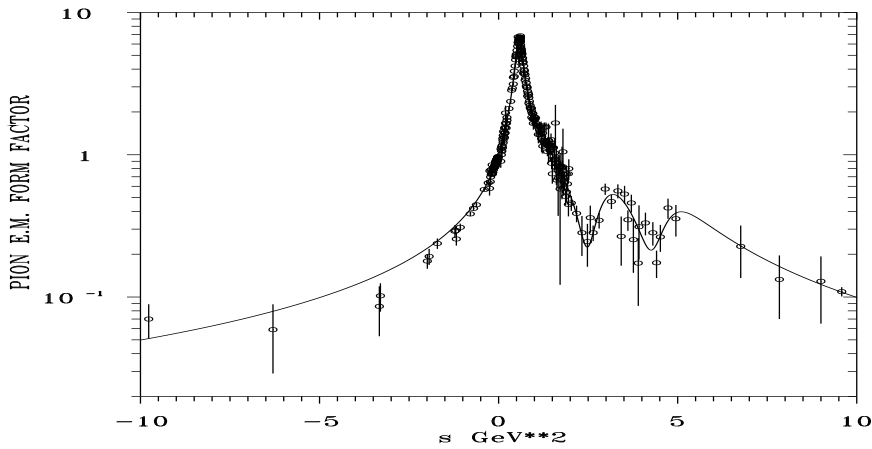


Figure 4:

5.3 Confirmation of $\rho'''(2150)$ from kaon electromagnetic form factors data

Similarly, the expression (28) can be used also for the isoscalar and isovector parts of the kaon electromagnetic FF's, to be saturated by isoscalar and isovector vector mesons, respectively. In a description of existing data, obtained from $e^+e^- \rightarrow K^+K^-$ (Fig. 5) and $e^+e^- \rightarrow K_S^0K_L^0$ (Fig. 6) processes, the isovector part of the kaon electromagnetic FF's was saturated by three rho-resonances. As a result, unlike the $e^+e^- \rightarrow \pi^+\pi^-$ process, the contribution of the $\rho'''(2150)$ is favored prior to the $\rho''(1700)$ by the data on charge and neutral kaon FF's.

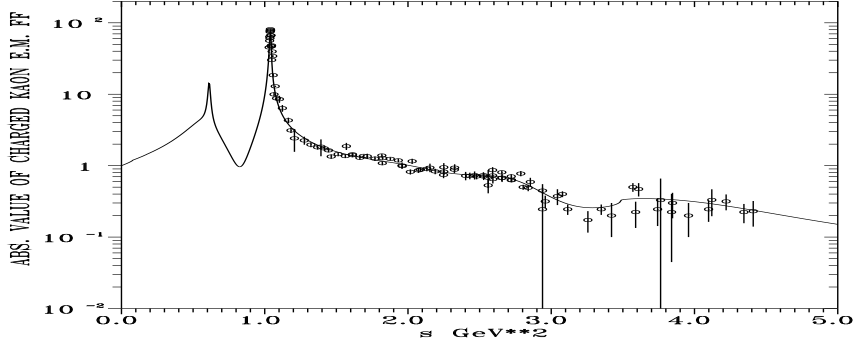


Figure 5:

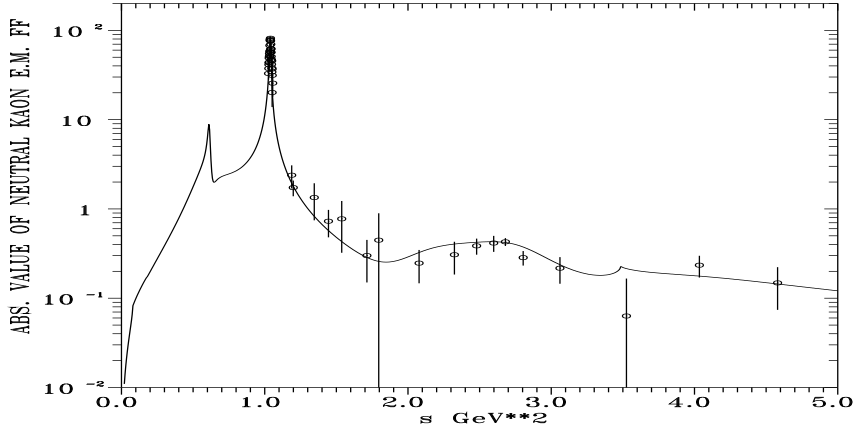


Figure 6:

5.4 Strange-quark vector-current form factor of K -mesons

Having unitary and analytic models of the kaon electromagnetic structure

$$F_K^{I=0}[V(t)] = \left(\frac{1-V^2}{1-V_N^2} \right)^2 \left\{ \frac{1}{2} H(V_{\omega'}) + [L(V_{\omega}) - H(V_{\omega'})] (f_{\omega KK}/f_{\omega}^e) + [L(V_{\phi}) - H(V_{\omega'})] (f_{\phi KK}/f_{\phi}^e) \right\} \quad (35)$$

$$F_K^{I=1}[W(t)] = \left(\frac{1-W^2}{1-W_N^2} \right)^2 \left\{ \frac{1}{2} H(W_{\rho''}) + [L(W_{\rho}) - H(W_{\rho''})] (f_{\rho KK}/f_{\rho}^e) + [L(W_{\rho'}) - H(W_{\rho''})] (f_{\rho' KK}/f_{\rho'}^e) \right\} \quad (36)$$

and the strange FF of kaon with the inner structure of $F_K^{I=0}[V(t)]$

$$F_K^S[V(t)] = \left(\frac{1-V^2}{1-V_N^2} \right)^6 \left\{ -H(V_{\omega'}) + [L(V_{\omega}) - H(V_{\omega'})] (f_{\omega KK}/f_{\omega}^s) + [L(V_{\phi}) - H(V_{\omega'})] (f_{\phi KK}/f_{\phi}^s) \right\} \quad (37)$$

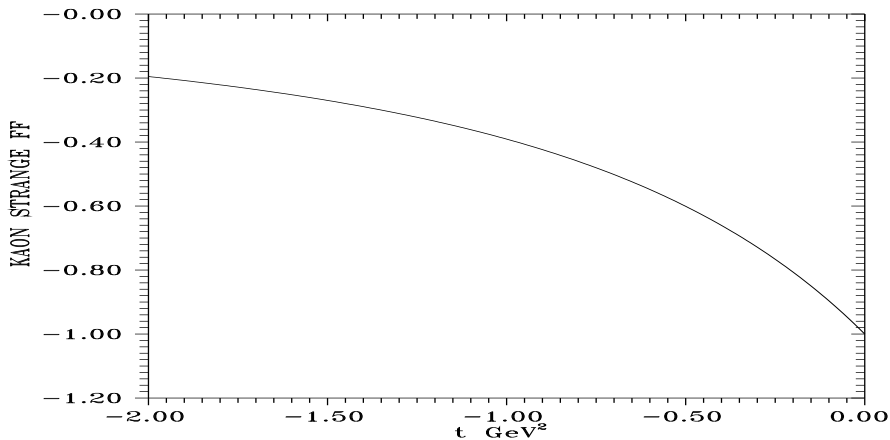


Figure 7:

set up, one can predict [5] a behaviour (see Figs. 7 - 9) of the strange FF of K -mesons (37) by means of the Jaffe's idea [6] of an evaluation of $(f_{\omega KK}/f_{\omega}^s)$, $(f_{\phi KK}/f_{\phi}^s)$ from $(f_{\omega KK}/f_{\omega}^e)$, $(f_{\phi KK}/f_{\phi}^e)$ determined in a comparison of (35) and (36) with data on charge and neutral kaon electromagnetic FF's.

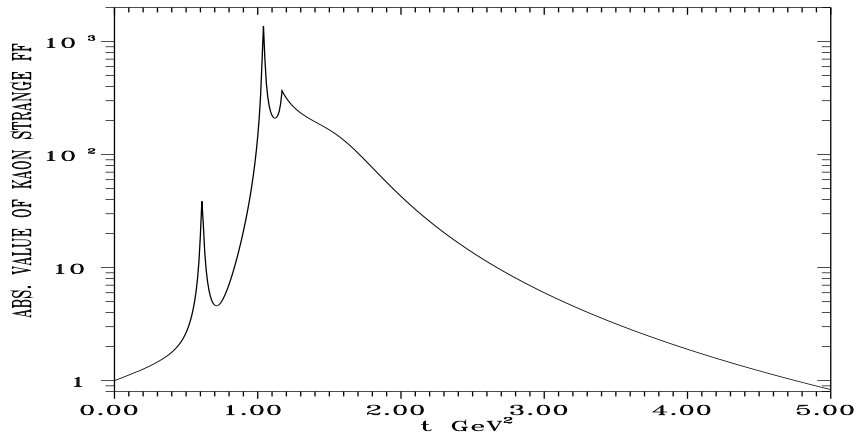


Figure 8:

5.5 Predictions for weak $\bar{\nu}_e e^- \rightarrow P^0 P^-$ and $\tau^- \rightarrow \nu_\tau P^0 P^-$ processes

The corresponding total cross-section (5) and the partial decay width expression (6) of the weak processes $\bar{\nu}_e e^- \rightarrow P^0 P^-$ and $\tau^- \rightarrow \nu_\tau P^0 P^-$, respectively, are completely determined by the weak FF's $F_P^W(s)$ ($P = \pi, K$).

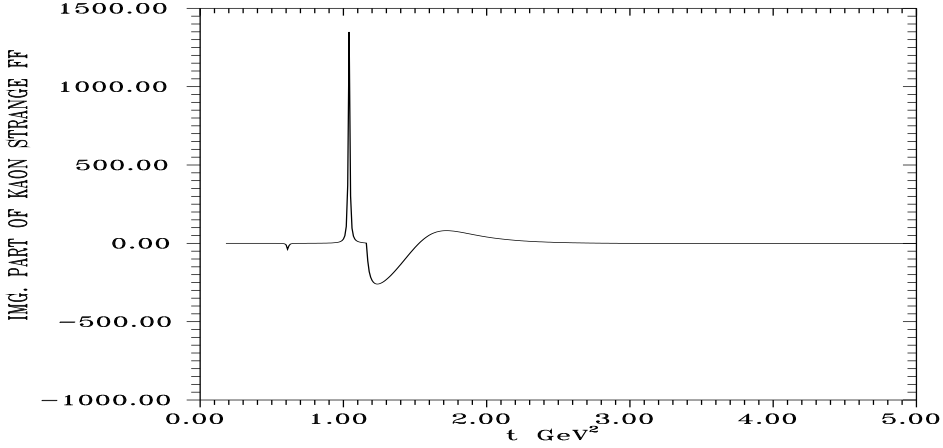


Figure 9:

In V-A theory of weak interactions the hadronic charged weak current takes the form

$$J_W^\mu = V^\mu + A^\mu. \quad (38)$$

On the other hand the electromagnetic current of hadrons has the form

$$J_E^\mu = J_3^\mu + J_s^\mu \quad (39)$$

where J_3^μ is a third component of the isotopic vector current $\vec{J}(J_1^\mu, J_2^\mu, J_3^\mu)$ and J_s^μ is an isoscalar current. Almost 50 years ago a very creative postulation was introduced [7, 8]

$$V^\mu = J_1^\mu - iJ_2^\mu \quad (40)$$

i.e. the charged weak vector current V^μ and J_3^μ of the electromagnetic current (39) are components of the same isotopic vector $\vec{J}(J_1^\mu, J_2^\mu, J_3^\mu)$. Because strong interactions are invariant according to the isotopic SU(2) group, then by $\vec{J}(J_1^\mu, J_2^\mu, J_3^\mu)$ the equation

$$\partial_\mu J_i^\mu = 0 \quad (41)$$

is fulfilled, from where the conserved-vector-current (CVC) hypothesis

$$\partial_\mu V^\mu = 0 \quad (42)$$

follows. Starting from eq. (42) one can prove the relation between the electromagnetic and weak pion FF's

$$F_\pi^W(s) = \sqrt{2}F_\pi^{E,I=1}(s) \quad (43)$$

and also the relation between weak kaon FF and the isovector part of the electromagnetic FF's of K -mesons

$$F_K^W(s) = 2F_K^{E,I=1}(s). \quad (44)$$

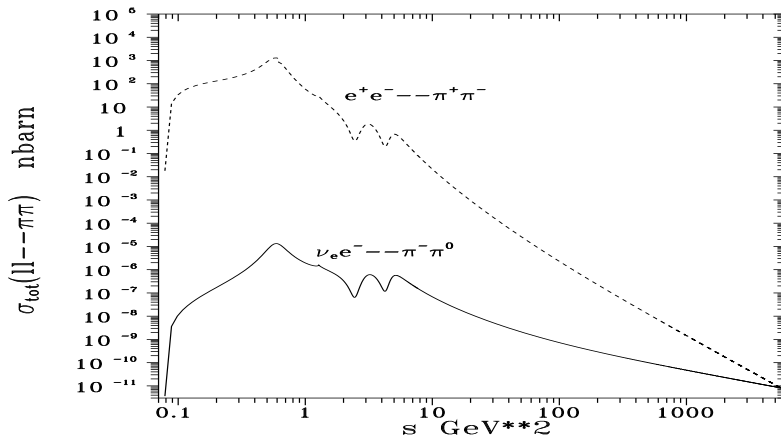


Figure 10:

If now for $F_{\pi}^{E,I=1}(s)$ and $F_K^{E,I=1}(s)$ unitary and analytic models of the type (28) are taken into account, by means of (43) and (44) behaviours of $F_{\pi}^W(s)$ and $F_K^W(s)$ are found and evaluations of physical quantities (5) and (6) are achieved.

Our theoretical predictions for branching ratios:	Exp. values of branching ratios from ALEPH in CERN:
$B(\tau^- \rightarrow \nu_{\tau} \pi^0 \pi^-) = 25.76\%$ [9]	$B(\tau^- \rightarrow \nu_{\tau} \pi^0 \pi^-) = 25.34 \pm 0.19\%$ [11]
$B(\tau^- \rightarrow \nu_{\tau} K^0 K^-) = 0.18\%$ [10]	$B(\tau^- \rightarrow \nu_{\tau} K^0 K^-) = 0.194 \pm 0.042\%$ [11]

For comparison of $\sigma_{\text{tot}}(\bar{\nu}_e e^- \rightarrow \pi^0 \pi^-)$ and $\sigma_{\text{tot}}(e^+ e^- \rightarrow \pi^+ \pi^-)$ see Fig. 10. For kaons can't be carried out such a comparison.

5.6 Unitary and analytic model of nucleon electromagnetic structure and its predictability

Keeping a procedure discussed at the end of the Section 4. one can construct ten-resonance (5 isoscalars and 5 isovectors) unitary and analytic model of nucleon electromagnetic structure [12], which describes well all existing experimental space-like and time-like data on the nucleon electromagnetic form factors, including also FERMILAB proton eight points [13, 14] at higher energies (see Fig. 11) and FENICE (Frascati) results [15] on the neutron (see Fig. 12), for the first time. The latter was achieved without any external constraints on the neutron charge radius and on the isovector spectral functions following from the πN -scattering data and pion electromagnetic form factor behaviour through the unitarity condition [16]. Just opposite, the model itself spontaneously predicts a negative value for the neutron charge radius and a pronounced effect of the two-pion continuum

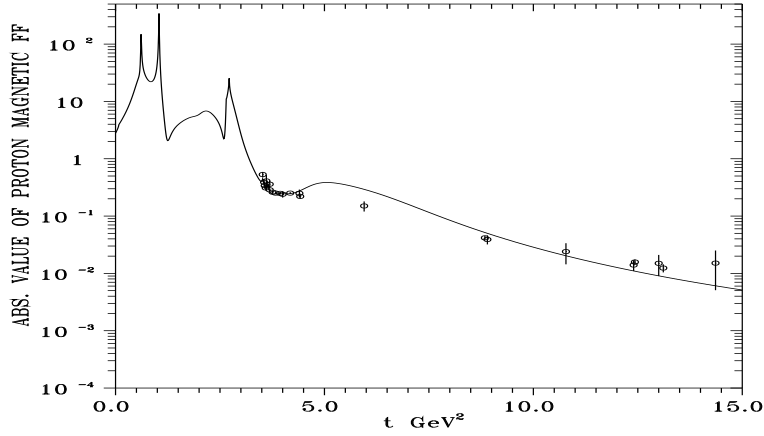


Figure 11:

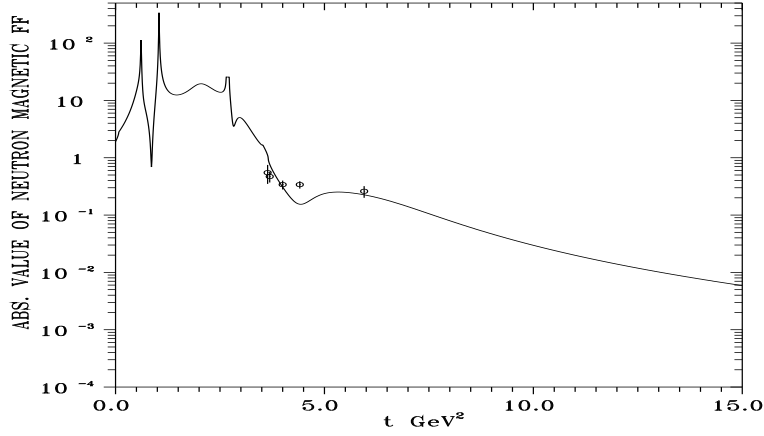


Figure 12:

on the isovector spectral functions (see Fig. 13) revealing the strong enhancement of the left wing of the $\rho(770)$ -resonance close to two-pion threshold. Moreover, an existence of the fourth excited state of the $\rho(770)$ meson at $t \approx 6.25 \text{ GeV}^2$, the large values of coupling constants $f_{\phi NN}^{(1)} = 12.1$ and $f_{\phi NN}^{(2)} = 3.4$ (indicating a violation of the OZI rule and a nonzero strange-quark content in nucleons) as well as the isoscalar spectral functions behaviours (see Fig. 14) are predicted by such a model.

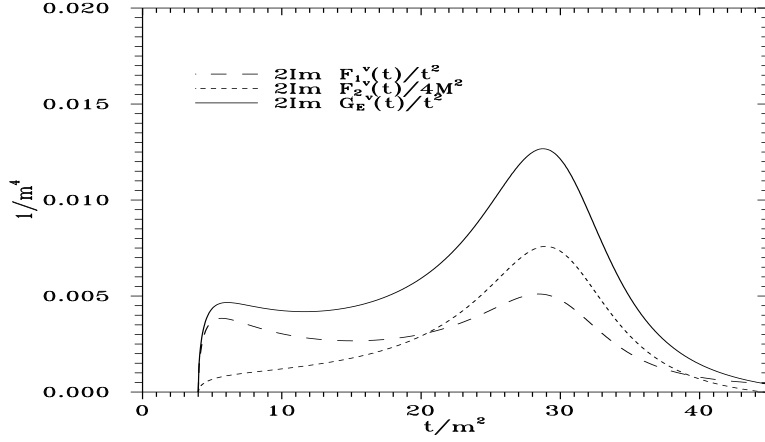


Figure 13:

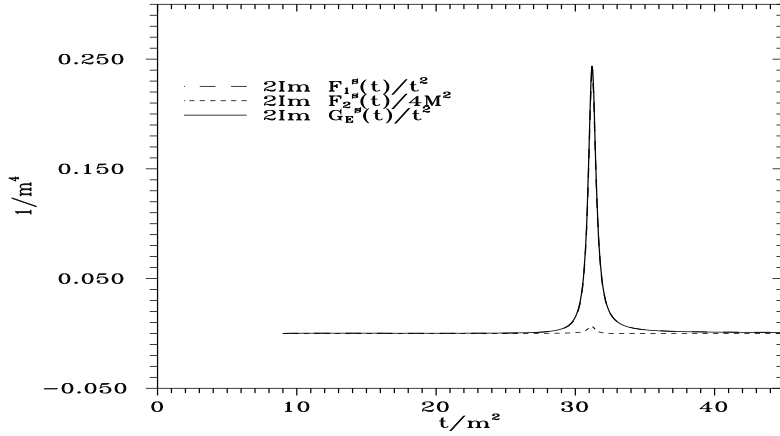


Figure 14:

5.7 Confirmation of strange-quark contributions to nucleon structure by the unitary and analytic model of nucleon electromagnetic FF's

More recently, a well-defined experimental program has just started determination of the nucleon matrix element

$$\langle p' | \bar{s} \gamma_\mu s | p \rangle = \bar{u}(p') \left[\gamma_\mu F_1^s(t) + i \frac{\sigma_{\mu\nu} q^\nu}{2 m_N} F_2^s(t) \right] u(p) \quad (45)$$

of the strange-quark vector current $\bar{s} \gamma_\mu s$ by means of the elastic scattering of polarized electron beam on liquid hydrogen target, in which (unlike the most theoretical estimates) unexpected positive values of strange FF's

$$G_E^s(t) = F_1^{(s)}(t) + \frac{t}{4m_N^2} F_2^{(s)}(t)$$

$$G_M^s(t) = F_1^{(s)}(t) + F_2^{(s)}(t) \quad (46)$$

were revealed:

the SAMPLE Collaboration at MIT/Bates Linear Accelerator Center [17]

$$G_M^s(-0.1) = +0.23 \pm 0.37 \pm 0.15 \pm 0.19 \quad [\mu_N] \quad (47)$$

or improved measurements at the same Center [18]

$$G_M^s(-0.1) = +0.61 \pm 0.17 \pm 0.21 \pm 0.19 \quad [\mu_N] \quad (48)$$

and the HAPPEX Collaboration at TJNAF [19]

$$G_E^s(-0.48) + 0.39G_M^s(-0.48) = +0.023 \pm 0.034 \pm 0.022 \pm 0.026. \quad (49)$$

If there are really nonzero strange nucleon FF's, then as a result of the isospin zero value of the strange quark, they can exclusively contribute just to isoscalar parts of the nucleon electromagnetic FF's and never to the isovector FF's. We show, that by specific eight resonance unitary and analytic model of the nucleon electromagnetic structure, the isoscalar part of which depends only on ω and ϕ coupling constant ratios as free parameters, one can explain all experimental results (47)-(49).

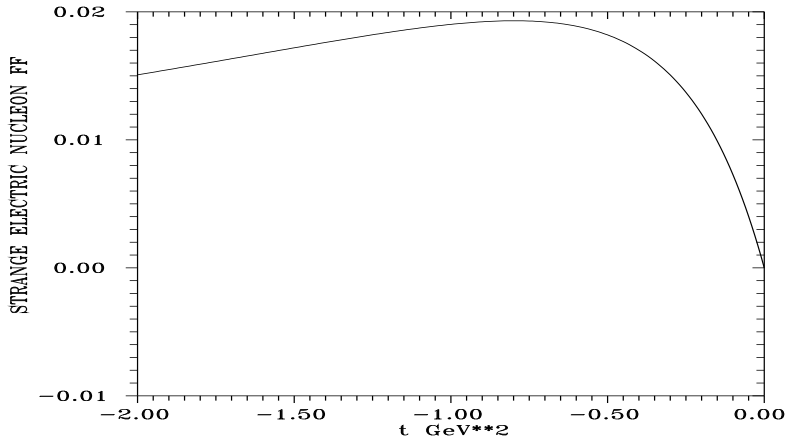


Figure 15:

The main idea of a prediction of strange nucleon FF behaviour, based on the $\omega - \phi$ mixing and on the assumption that the quark current of some flavour couples with universal strength exclusively to the vector-meson wave function component of the same

flavour, consists in the following. Provided that one knows free parameters $(f_{\omega NN}^{(i)}/f_{\omega}^e)$, $(f_{\phi NN}^{(i)}/f_{\phi}^e)$ of the unitary and analytic model

$$F_i^{I=0}(t) = f[t; (f_{\omega NN}^{(i)}/f_{\omega}^e), (f_{\phi NN}^{(i)}/f_{\phi}^e)] \quad (i = 1, 2) \quad (50)$$

then the unknown free parameters $(f_{\omega NN}^{(i)}/f_{\omega}^s)$, $(f_{\phi NN}^{(i)}/f_{\phi}^s)$ of a strange nucleon FF's unitary and analytic model

$$F_i^s(t) = \bar{f}[t; (f_{\omega NN}^{(i)}/f_{\omega}^s), (f_{\phi NN}^{(i)}/f_{\phi}^s)] \quad (i = 1, 2) \quad (51)$$

of the same inner analytic structure as $F_i^{I=0}(t)$, but of course with different norm and possibly with different asymptotics (therefore denoted by \bar{f}), are numerically evaluated by the relations [6]

$$(f_{\omega NN}^{(i)}/f_{\omega}^s) = -\sqrt{6} \frac{\sin \varepsilon}{\sin(\varepsilon + \theta_0)} (f_{\omega NN}^{(i)}/f_{\omega}^e) \quad (i = 1, 2) \quad (52)$$

$$(f_{\phi NN}^{(i)}/f_{\phi}^s) = -\sqrt{6} \frac{\cos \varepsilon}{\cos(\varepsilon + \theta_0)} (f_{\phi NN}^{(i)}/f_{\phi}^e)$$

where $\varepsilon = 3.7^\circ$ is a deviation from the ideally mixing angle $\theta_0 = 35.3^\circ$.

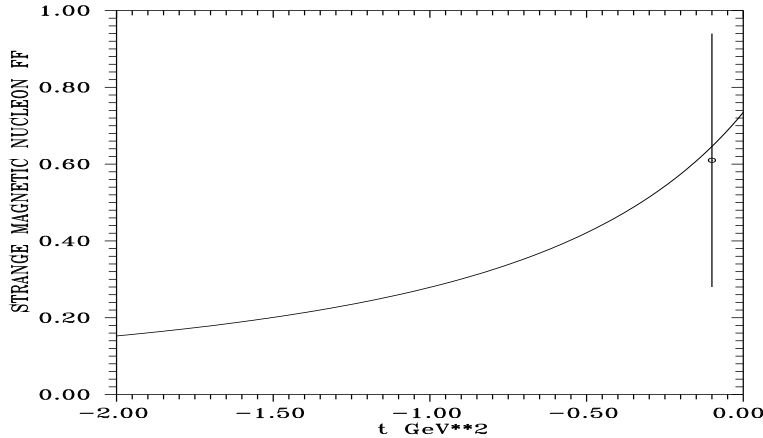


Figure 16:

The parameters $(f_{\omega NN}^{(i)}/f_{\omega}^e)$, $(f_{\phi NN}^{(i)}/f_{\phi}^e)$ ($i = 1, 2$) were evaluated by a comparison of the eight resonance unitary and analytic model (50) with existing data, then $(f_{\omega NN}^{(i)}/f_{\omega}^s)$, $(f_{\phi NN}^{(i)}/f_{\phi}^s)$ were calculated by means of (52) and behaviour of $G_E^s(t)$, $G_M^s(t)$ was predicted [20] as it is presented in Figs. 15 and 16. One can see from Fig. 16 that the improved SAMPLE collaboration result (48) is preferred to the older one (47) and that

the strange magnetic moment of the nucleon is positive valued to be $\mu_s = G_M^s(0) = F_2^s(0) = +0.73 [\mu_N]$. On the other hand one obtains

$$G_E^s(-0.48) + 0.39 G_M^s(-0.48) = +0.185 \quad (53)$$

indicating also the positive value like in (49). The behaviours of $G_E^s(t)$, $G_M^s(t)$ give also a prediction for a combination

$$G_E^s(-0.23) + 0.22 G_M^s(-0.23) = +0.135 \quad (54)$$

which is just measured at the MAMI A4 [21] running experiment.

5.8 Prediction of $\sigma_{\text{tot}}(e^+e^- \rightarrow Y\bar{Y})$ behaviour

According to SU(3) classification of hadrons there is $1/2^+$ octet of baryons including nucleon doublet $[n, p]$ together with 6 other hyperons $[\Lambda^0]$, $[\Sigma^+, \Sigma^0, \Sigma^-]$ and $[\Xi^0, \Xi^-]$. Though there is almost zero experimental information on the hyperon electromagnetic structure, by using the unitary and analytic models of electromagnetic FF's of all members of the $1/2^+$ octet of baryons, the experimental information on the nucleon electromagnetic FF's and SU(3) symmetry, one can predict behaviours of the hyperon electromagnetic FF's and as a result also behaviours of

$$\sigma_{\text{tot}}(e^+e^- \rightarrow Y\bar{Y}) = \frac{4\pi\alpha^2\beta_Y}{3t} \left[|G_M^Y(t)|^2 + \frac{2m_Y^2}{t} |G_E^Y(t)|^2 \right]. \quad (55)$$

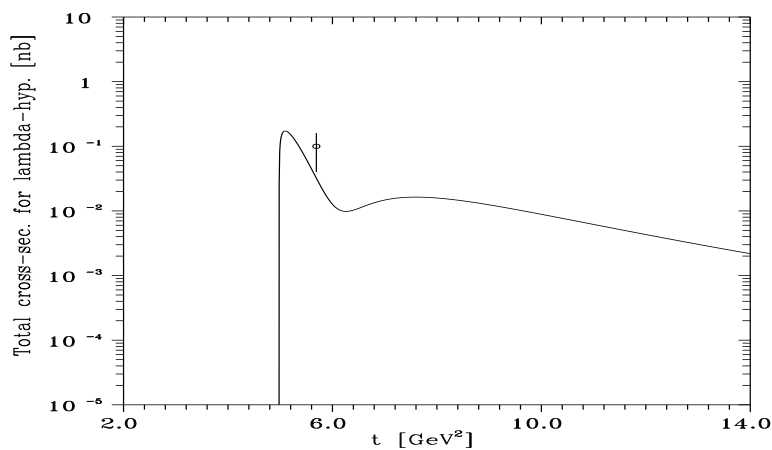


Figure 17:

Practically, one has to start with a specific nine resonance unitary and analytic model of the electromagnetic FF's of $1/2^+$ octet of baryons, unifying compatibly all known

properties of FF's, which renders just ρ -, ω - and ϕ -meson coupling constant ratios as free parameters.

For nucleons, these free parameters are evaluated numerically by a comparison of the nucleon model with existing nucleon FF data and then it is straightforward to find numerical values of $f_{\rho NN}$, $f_{\omega NN}$ and $f_{\phi NN}$.

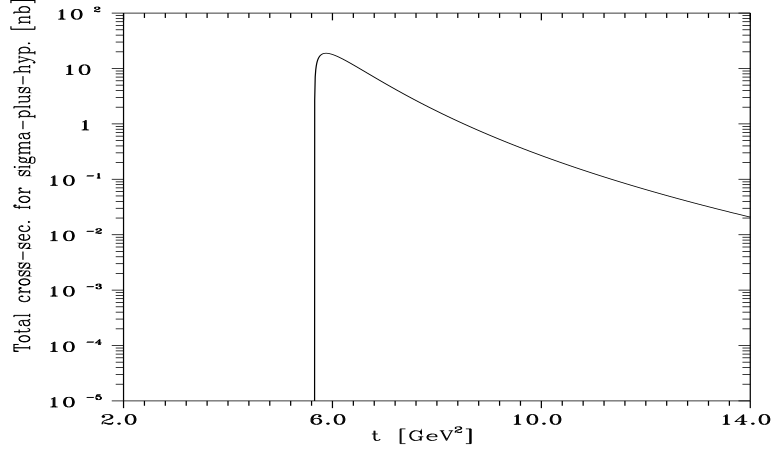


Figure 18:

On the other hand, the trace of SU(3) invariant Lagrangian for vector-meson-baryon-antibaryon vertex

$$\begin{aligned}
\text{Tr}(L_{V\bar{B}B}) &= \frac{i}{\sqrt{2}} f^F \left[\bar{B}_\beta^\alpha \gamma_\mu B_\gamma^\beta - \bar{B}_\gamma^\beta \gamma_\mu B_\beta^\alpha \right] (V_\mu)_\alpha^\gamma + \\
&+ \frac{i}{\sqrt{2}} f^D \left[\bar{B}_\gamma^\beta \gamma_\mu B_\beta^\alpha + \bar{B}_\beta^\alpha \gamma_\mu B_\gamma^\beta \right] (V_\mu)_\alpha^\gamma + \\
&+ \frac{i}{\sqrt{2}} f^S \bar{B}_\beta^\alpha \gamma_\mu B_\alpha^\beta \omega_\mu^0
\end{aligned} \tag{56}$$

with $\omega - \phi$ mixing

$$\begin{aligned}
\phi^0 &= \phi_8 \cos \vartheta - \omega_1 \sin \vartheta \\
\omega^0 &= \phi_8 \sin \vartheta + \omega_1 \cos \vartheta
\end{aligned} \tag{57}$$

B, \bar{B} and V baryon, antibaryon and vector-meson octuplet matrices, ω_μ^0 omega-meson singlet, f^F , f^D and f^S SU(3) coupling constants and ϑ mixing angle, provides the following expressions for vector-meson-baryon coupling constants

$$\begin{aligned}
f_{\rho NN}^{(1,2)} &= \frac{1}{2} (f_{1,2}^D + f_{1,2}^F) \\
f_{\omega NN}^{(1,2)} &= \frac{1}{\sqrt{2}} \cos \vartheta f_{1,2}^S - \frac{1}{2\sqrt{3}} \sin \vartheta (3f_{1,2}^F - f_{1,2}^D) \\
f_{\phi NN}^{(1,2)} &= \frac{1}{\sqrt{2}} \sin \vartheta f_{1,2}^S + \frac{1}{2\sqrt{3}} \cos \vartheta (3f_{1,2}^F - f_{1,2}^D)
\end{aligned} \tag{58}$$

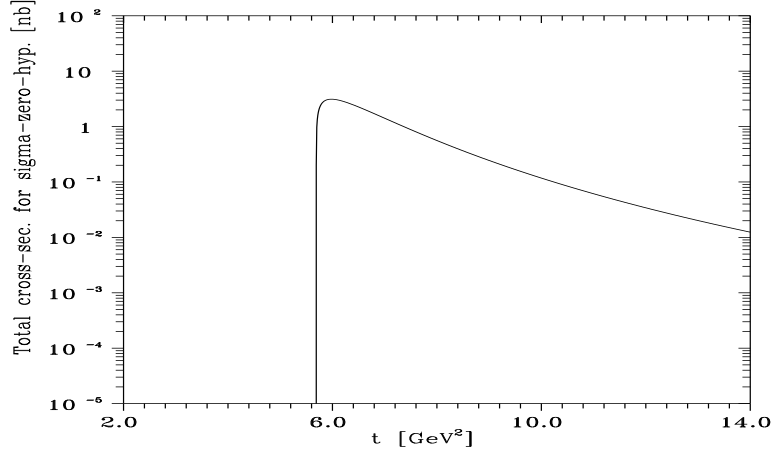


Figure 19:

$$f_{\omega\Lambda\Lambda}^{(1,2)} = \frac{1}{\sqrt{2}} \cos \vartheta f_{1,2}^S + \frac{1}{\sqrt{3}} \sin \vartheta f_{1,2}^D \quad (59)$$

$$f_{\phi\Lambda\Lambda}^{(1,2)} = \frac{1}{\sqrt{2}} \sin \vartheta f_{1,2}^S - \frac{1}{\sqrt{3}} \cos \vartheta f_{1,2}^D$$

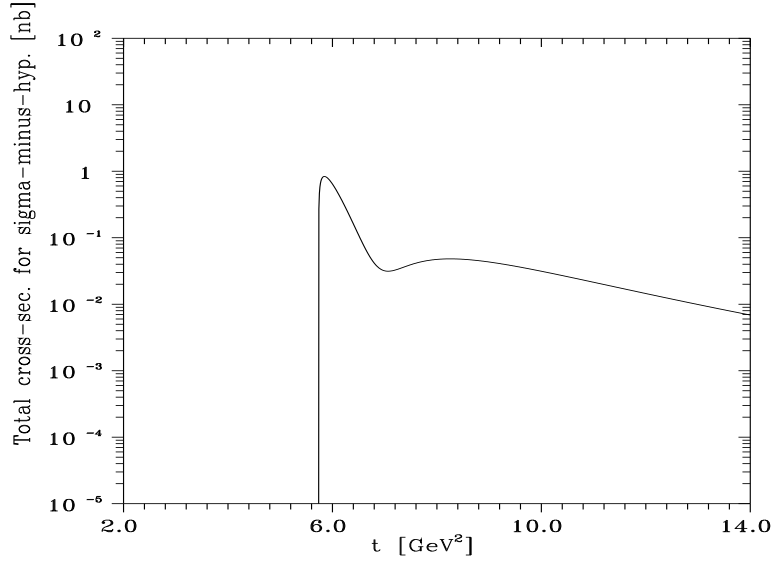


Figure 20:

$$f_{\rho\Sigma\Sigma}^{(1,2)} = -f_{1,2}^F$$

$$f_{\omega\Sigma\Sigma}^{(1,2)} = \frac{1}{\sqrt{2}} \cos \vartheta f_{1,2}^S - \frac{1}{\sqrt{3}} \sin \vartheta f_{1,2}^D \quad (60)$$

$$f_{\phi\Sigma\Sigma}^{(1,2)} = \frac{1}{\sqrt{2}} \sin \vartheta f_{1,2}^S + \frac{1}{\sqrt{3}} \cos \vartheta f_{1,2}^D$$

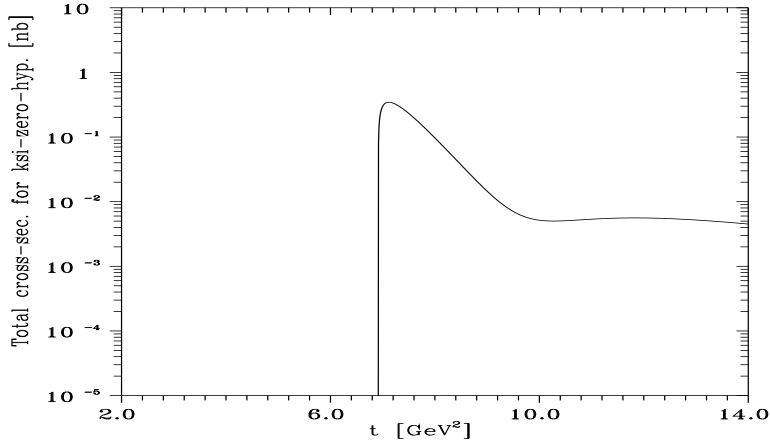


Figure 21:

$$\begin{aligned}
 f_{\rho \Xi \Xi}^{(1,2)} &= \frac{1}{2}(f_{1,2}^D - f_{1,2}^F) \\
 f_{\omega \Xi \Xi}^{(1,2)} &= \frac{1}{\sqrt{2}} \cos \vartheta f_{1,2}^S + \frac{1}{2\sqrt{3}} \sin \vartheta (3f_{1,2}^F + f_{1,2}^D) \\
 f_{\phi \Xi \Xi}^{(1,2)} &= \frac{1}{\sqrt{2}} \sin \vartheta f_{1,2}^S - \frac{1}{2\sqrt{3}} \cos \vartheta (3f_{1,2}^F + f_{1,2}^D).
 \end{aligned} \tag{61}$$

Then the solutions of the system of algebraic eqs. (58) according to $f_{1,2}^D$, $f_{1,2}^F$, $f_{1,2}^S$ with numerical values of $f_{\rho NN}^{1,2}$, $f_{\omega NN}^{1,2}$ and $f_{\phi NN}^{1,2}$, enable by means of the expressions (59)-(61) to predict all free vector-meson-hyperon coupling constant ratios in the electromagnetic FF's of hyperons $[\Lambda^0]$, $[\Sigma^+, \Sigma^0, \Sigma^-]$ and $[\Xi^0, \Xi^-]$ and, as a result, also behaviours of the total cross-sections (55) (see Figs. 17-22).

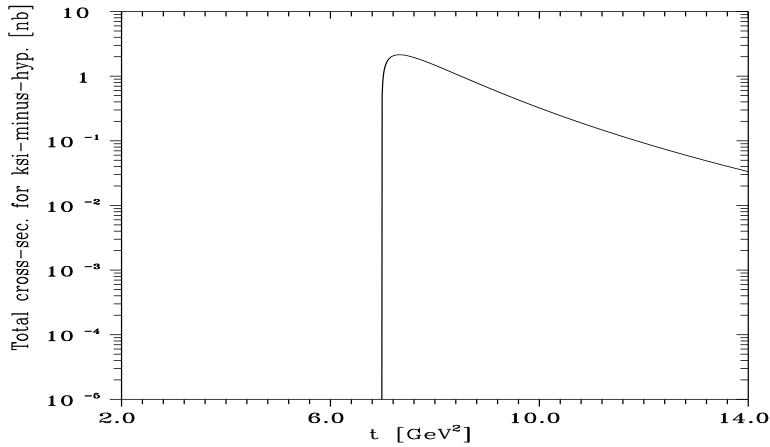


Figure 22:

5.9 Estimation of hadronic contributions to the anomalous magnetic moment of the muon with higher precision

Charged leptons ($l = e^-, \mu^-, \tau^-$) are described by the Dirac equation and their magnetic moments are related to the spin by the relation

$$\mu_l = g_l \frac{e}{2m_l} \frac{\hbar}{2c} \quad (62)$$

where the value of the gyromagnetic ratio g_l is predicted (in the absence of the Pauli term) to be exactly 2.

Practically, however, the interactions existing in nature modify g_l to be different from 2 because of the emission and absorption of virtual photons (electromagnetic effects), intermediate vector and Higgs bosons (weak interaction effects) and the vacuum polarization into virtual hadronic states (strong interaction effects).

In order to describe theoretically this modification of g_l , the magnetic anomaly was introduced by the relation

$$a_l \equiv \frac{g_l - 2}{2} = a_l^{(1)} \cdot \frac{\alpha}{\pi} + (a_l^{(2) QED} + a_l^{(2) had}) \cdot \left(\frac{\alpha}{\pi}\right)^2 + a_l^{(2) weak} + O\left(\frac{\alpha}{\pi}\right)^3 \quad (63)$$

where $\alpha = 1/137.0359895(61)$ is the fine-structure constant.

From all three leptons the most interesting for theoretical investigations is the muon magnetic anomaly a_μ :

- it is one of the best measured quantities in physics

$$a_\mu^{\text{exp}} = (116\,592\,290 \pm 850) \times 10^{-11} \quad [22] \quad (64)$$

- its accurate theoretical evaluation provides an extremely clean test of "Electroweak theory" and may give hints on possible deviations from STANDARD MODEL (SM).
- the NEW E-821 experiment [23] in Brookhaven National Laboratory (BNL) is under way, which is expected to be performed with an accuracy

$$\Delta a_\mu^{\text{exp}} = \pm 43 \times 10^{-11}. \quad (65)$$

i.e. it is aimed at obtaining a factor of 20 in a precision above that of the previous CERN measurements (64).

Comparing theoretical evaluations of QED, WEAK and STRONG effects

QED:

$$a_{\mu}^{\text{QED}} = (116584694.7 \pm 4.6) \times 10^{-11} \quad (\text{KNO}) [24] \quad (66)$$

$$a_{\mu}^{\text{QED}} = (116584698.4 \pm 1.7) \times 10^{-11} \quad (\text{K}) [25]$$

WEAK:

$$a_{\mu}^{\text{W}} = (155.1 \pm 2.7) \times 10^{-11} \quad (\text{PPdeR}) [26] \quad (67)$$

$$a_{\mu}^{\text{W}} = (152 \pm 3 \pm 0.45\text{R}_b) \times 10^{-11} \quad (\text{CzKM}) [27]$$

STRONG:

$$\begin{aligned} a_{\mu}^{\text{had}} &= (7068 \pm 172) \times 10^{-11} \quad (\text{KNO}) [28] \\ a_{\mu}^{\text{had}} &= (7100 \pm 116) \times 10^{-11} \quad (\text{CLY}) [29] \\ a_{\mu}^{\text{had}} &= (7024 \pm 152) \times 10^{-11} \quad (\text{EJ}) [30] \end{aligned} \quad (68)$$

it is straightforward to see, that the largest uncertainty comes from STRONG interaction contributions (68). Their errors are comparable with central values of WEAK interaction effects in (67).

So, if one would like to test the SM predictions for a_{μ}^{W} , possibly to obtain hints for physics beyond SM, one has still to lower the error of a_{μ}^{had} .

The latter quantity can be represented by the integral

$$a_{\mu}^{(2)\text{had}} = \frac{1}{4\pi^3} \int_{4m_{\pi}^2}^{\infty} \sigma^h(s) K_{\mu}^{(2)}(s) ds \quad (69)$$

where

$$\begin{aligned} \sigma^h(s) \equiv \sigma_{\text{tot}}(e^+e^- \rightarrow \text{had}) &= \sigma_{\text{tot}}(e^+e^- \rightarrow \pi^+\pi^-) + \sigma_{\text{tot}}(e^+e^- \rightarrow K^+K^-) + \\ &+ \sigma_{\text{tot}}(e^+e^- \rightarrow K^0\bar{K}^0) + \sigma_{\text{tot}}(e^+e^- \rightarrow \pi^+\pi^-\pi^0) + \dots \end{aligned} \quad (70)$$

and

$$K_{\mu}^{(2)}(s) = \int_0^1 \frac{x^2(1-x)}{x^2 + (1-x)s/m_{\mu}^2} dx. \quad (71)$$

From the practical point of view it was advantageous to separate the low energy ($4m_\pi^2 < s < s_0$) from the high energy region ($s_0 < s < \infty$) in the integral (69) as follows

$$a_\mu^{(2)\text{ had}} = \frac{1}{4\pi^3} \left\{ \int_{4m_\pi^2}^{s_0} \left[\sum_F \sigma_{\text{tot}}(e^+e^- \rightarrow F) \right] K_\mu^{(2)}(s) ds + \int_{s_0}^{\infty} R(e^+e^- \rightarrow \text{had}) \sigma_{\text{tot}}(e^+e^- \rightarrow \mu^+\mu^-) K_\mu^{(2)}(s) ds \right\}. \quad (72)$$

The s_0 was fixed at 2 GeV², where an overlapping region of the data on total cross-sections of exclusive processes $e^+e^- \rightarrow F$ and the data on $R = \sigma_{\text{tot}}(e^+e^- \rightarrow \text{had})/\sigma_{\text{tot}}(e^+e^- \rightarrow \mu^+\mu^-)$ already exists.

Then the first error lowering in a_μ^{had} was achieved in [31]

$$a_\mu^{\text{had}} = (7052 \pm 76) \times 10^{-11} \quad (73)$$

where instead of an integration over the experimental data on the first three total cross-sections in (70) refined models of the corresponding FF's were used and for a determination of their free parameters not only the data of the region of a definition of $\sigma_{\text{tot}}(e^+e^- \rightarrow P\bar{P})$ ($P = \pi, K$), but all existing space-like and time-like data, were used.

Even better error lowering in a_μ^{had} was reached in [32]

$$a_\mu^{\text{had}} = (6986 \pm 45) \times 10^{-11} \quad (74)$$

if for the corresponding FF's the sophisticated unitary and analytic models, discussed in Sect. 4, were applied. Really, in this case the error is diminished down to one fourth of the WEAK interaction contribution (67) and becomes comparable with the accuracy (65) expected in the new $g - 2$ muon running experiment at BNL [23].

6 Conclusions

We have formulated main principles of the unitary and analytic models of the electromagnetic structure of hadrons and nuclei. Then a general scheme of their utilization to the electromagnetic, weak and strong interaction processes was traced out. Finally, their practical application for a description of the electromagnetic and weak FF's, by means of which a lot of interesting results were obtained, convinces us that they are still powerful tools in the particle physics phenomenology.

7 Acknowledgements

The work was partly supported by Slovak Grant Agency for Sciences, Grant No. 2/5085/2000 (S.D. and P.S.) and Grant No. 1/7068/2000 (A.Z.D.).

References

- [1] S.Dubnička, A.Z.Dubničková, P. Stríženec, *Nuovo Cim.* **A106**, 1993, 1253.
- [2] S. Dubnička, Ľ. Martinovič, *Lett. Nuovo Cim.* **44**, 1985, 462.
- [3] S. Dubnička, Ľ. Martinovič: *Proc. XXI. Recontre de Moriond : Strong Interactions and Gauge Theories*, March 16-22, 1986, Ed.: J. Tran Thanh Van, Frontières, Gif sur Yvette (1986) p. 297.
- [4] M.E. Biagini, S. Dubnička, E. Etim, P. Kolář, *Nuovo Cim.* **A104**, 1991, 363.
- [5] M. Anselmino, S. Dubnička, A.Z. Dubničková: *Frascati Physics Series Vol. XVI: Physics and detectors for DAΦNE*, Frascati (2000), p. 477.
- [6] R.L. Jaffe, *Phys. Lett.* **229B**, 1989, 275.
- [7] S.S. Gerstein, Ya.B. Zeldovich, *ZhETP* **29**, 1955, 698.
- [8] R.P. Feynman, M. Gell-Mann, *Phys. Rev.* **109**, 1958, 193.
- [9] S. Dubnička, A.Z. Dubničková, A. Antušek, *Acta Phys. Slovaca* **49**, 1999, 165.
- [10] A.Z. Dubničková: *Doctor of Sciences (DrSc)Thesis*, JINR Dubna (1997).
- [11] D. Buskulic et. al., *Z. Phys.* **C70**, 1996, 579.
- [12] S. Dubnička, A.Z. Dubničková, P. Weisenpacher, hep-ph/0001240, 24. Jan. 2000.
- [13] T.A. Armstrong et. al., *Phys. Rev. Lett.* **70**, 1993, 1212.
- [14] M. Ambrogioni et al., *Phys. Rev.* **D60**, 1999, 032002-1.
- [15] A. Antonelli et al., *Nucl. Phys.* **B517**, 1998, 3.
- [16] G. Höhler, E. Pietarinen, *Phys. Lett.* **53B**, 1975, 471.
- [17] M. Mueller et al., SAMPLE Collaboration, *Phys. Rev. Lett.* **78**, 1997, 3824.
- [18] D.T. Spayde et al., SAMPLE Collaboration, *Phys. Rev. Lett.* **84**, 2000, 1106.
- [19] K.A. Aniol et al., HAPPEX Collaboration, *Phys. Rev. Lett.* **82**, 1999, 1096.
- [20] S. Dubnička, A.Z. Dubničková, P. Weisenpacher, hep-ph/0102171, 14. Feb. 2001.

- [21] MAMI A4 Collaboration, D. von Harrach et al. (unpublished).
- [22] F.J.M. Farley, *Z. Phys.* **C56**, 1992, S 88.
- [23] B.Lee Roberts, *Z. Phys.* **C56**, 1992, S 101.
- [24] T. Kinoshita, B. Nizić, Y. Okamoto, *Phys. Rev.* **D41**, 1990, 593.
- [25] T. Kinoshita, *Cornell Univ. Preprint*, CLNS 93/1187, Ithaca (1993).
- [26] S. Peris, M. Perrotel, E.de Rafael, CERN-TH/95-141.
- [27] A. Czarnecki, B. Krause, W.J. Marciano, *Phys. Rev.* **D52**, 1995, R2619.
- [28] T. Kinoshita, B. Nizić, Y. Okamoto, *Phys. Rev.* **D31**, 1985, 2108.
- [29] J.A. Casas, C. Lopéz, F.J. Ynduráin, *Phys. Rev.* **D32**, 1985, 736.
- [30] S. Eidelman, F. Jegerlehner, *Z. Phys.* **C67**, 1995, 585.
- [31] Ľ. Martinovič, S. Dubnička, *Phys. Rev.* **D42**, 1990, 884.
- [32] A.Z. Dubničková, S. Dubnička, P. Stríženec, *Acta Phys. Slovaca* **45**, 1995, 467.